2

Light-Induced Dynamic Gratings and Photorefraction

Hans Joachim Eichler and Andreas Hermerschmidt

TU Berlin, Institute of Optics, Straße des 17. Juni 135, 10623 Berlin, Germany
eichler@physik.tu-berlin.de

2.1 Introduction

The spatial superposition of two or more coherent light waves yields a spatially modulated distribution of the energy density, and the interaction with the material leads to the creation of light-induced dynamic gratings. Many interesting effects and applications are based on such gratings. In some applications, e.g. when using dynamic gratings for holographic storage applications [1, 2] or the nanofabrication of three-dimensional photonic crystals by holographic lithography [3], the superposition of the beams defines the spatial structure of the grating. In other applications like using Stimulated Brillouin Scattering (SBS) for the creation of phase-conjugating mirrors for high-power laser systems [4, 5], the superposition of the laser beam with initially randomly scattered beam components eventually leads to the build-up of a dynamic grating acting as a phase-conjugating mirror.

The photorefractive effect, which is the topic of this volume, is as well based on dynamic light-induced gratings and has many applications and very interesting properties. For example, phase-conjugating mirrors based on Four-Wave Mixing in photorefractive materials do not have a distinct threshold in terms of laser intensity due to the entirely different physical process of the grating creation [6, 7] in contrast to the previously mentioned case of mirrors based on SBS. However, it is interesting that beam fanning as a driving effect for the build-up of such a photorefractive mirror [8] is again based on the transient evolution of scattered beam components, like in the SBS case.

Following a similar approach to the topic as used in [9] in this chapter, we will first recapitulate some basic properties of coherent light fields, which are usually derived from lasers [10], and discuss two-beam interference leading to interference gratings. In Section 2.3, we will discuss how the material response leads to changes in the absorption and the refraction of the material, which are described as amplitude and phase gratings. The diffraction of light at the gratings and wave mixing effects are described in Section 2.4.

2.2 Two-Beam Interference and Interference Gratings

Many properties of laser beams related to dynamic grating physics and applications can be described by a plane-wave approximation of the light field. The propagation of light in different types of media, the interference of light fields, and the diffraction of light at periodic structures are also often described using plane waves as a representation of the light field [11–13]. We will mainly follow the same approach, but we will also discuss some deviations of real laser beams from ideal plane waves, e.g., with respect to their limited size, duration, and coherence.

2.2.1 Plane Waves and Gaussian Laser Beams

In many experimental configurations, a Gaussian beam corresponding to the fundamental TEM_{00} mode of a laser resonator is used, which comes close to the ideal plane wave,

$$E(r, t) = A \exp[i(k \cdot r - \omega t + \phi)]. \tag{2.1}$$

Here E is the complex electric field vector dependent on the spatial coordinate r and time t, A the real-valued wave amplitude, k its wave vector, $\omega = 2\pi f$ its angular frequency, and ϕ a constant phase offset. The electric field E^r is given by

$$E^r(r, t) = \frac{1}{2}(E(r, t) + E^*(r, t)) = A \cos(k \cdot r - \omega t + \phi), \tag{2.2}$$

and can only take real values in order to retain its physical meaning [14]. For many computations, however, it is convenient to use the complex-valued field E (i.e., without adding the c.c.), but by doing so, the formulas for the relevant quantities can be slightly different from the familiar form.

The time-averaged Poynting vector S of a plane wave using complex-valued fields is given by [12]

$$S = \frac{1}{2}\mathrm{Re}(E \times H^*). \tag{2.3}$$

For the intensity I of this plane wave at point r, time t, given by the time average of the absolute value of the Poynting vector, we obtain

$$I(r, t) = \overline{|S|} = \frac{\varepsilon_0 cn}{2}|E(r, t)|^2 = \frac{1}{2Z}|E(r, t)|^2, \tag{2.4}$$

where c is the velocity of light, ε_0 the vacuum permittivity, n the refractive index, and $Z = \sqrt{\mu_r \mu_0 / \varepsilon_r \varepsilon_0}$ the corresponding wave resistance of the material. For most materials relevant in optics, the relative magnetic permeability μ_r is

given by $\mu_r \approx 1$, and the material properties are determined by the electric permittivity $\varepsilon = \varepsilon_0 \varepsilon_r$. To account for absorption and dispersion effects in isotropic materials with one quantity, the complex permittivity

$$\varepsilon_r = \varepsilon' + i\varepsilon''. \tag{2.5}$$

is introduced. Assuming weak absorption ($\varepsilon'' \ll \varepsilon'$), the complex-valued refractive index $\hat{n}$ is given by

$$\hat{n} = \sqrt{\varepsilon_r} \approx \sqrt{\varepsilon'} + i\frac{\varepsilon''}{2\sqrt{\varepsilon'}}. \tag{2.6}$$

The absorption coefficient α is introduced as

$$\alpha = \frac{2\omega}{c}\mathrm{Im}(\hat{n}) \approx \frac{\omega\varepsilon''}{nc}, \tag{2.7}$$

where $n = \mathrm{Re}(\hat{n})$ is the familiar real refractive index used in Eq. 2.4.

The electromagnetic energy density associated with the electric field E is given by

$$w(r, t) = \frac{1}{2}\varepsilon_0 \varepsilon' E(r, t) \cdot E^*(r, t). \tag{2.8}$$

Often, the interaction of the field with the material (i.e., the creation of a material excitation grating, see Section 2.3) is related to the rate of the dissipated energy density of the field that is given by [15]

$$W_f(r, t) = \frac{\varepsilon_0 \varepsilon'' \omega}{2} E(r, t) \cdot E^*(r, t). \tag{2.9}$$

For a plane wave and in isotropic materials, the rate of the dissipated energy density W_f and also the energy density w are directly proportional to the intensity as defined in Eq. 2.4

$$W_f(r, t) = \frac{\varepsilon_0 cn\alpha}{2} |E(r, t)|^2 = \alpha I(r, t). \tag{2.10}$$

Please note that while the left part of this equation is a general expression for weakly absorbing isotropic media, the right part obtained using Eq. 2.4 is valid for plane waves, but does not hold always in the general case.

In anisotropic materials, the permittivity of the material is described by introduction of the permittivity tensor ε_r. The resulting anisotropy of the refractive index is referred to as birefringence and in the case of uniaxial optical materials the propagation can be described using polarization-dependent refractive indices n_e and n_o for a given direction of the wave vector of the light. In some materials the anisotropy of the energy dissipation (referred to as dichroism) is also relevant.

The most relevant quantities describing the field in vacuum and within weakly absorbing materials are summarized in the Table 2.1. The expressions for the intensity are obtained for a single plane wave, while the other expressions are valid for general fields as well. In anisotropic materials, $\varepsilon_r, \varepsilon'$ and ε'' are tensor quantities. For the description of some effects, more sophisticated quantities may be needed to cover material properties like e.g., the polarization dependent quantum efficiency of the excitation processes involved [16].

In contrast to a plane wave, the amplitude of a field describing a laser beam is not constant within the plane of a wave front. A TEM_{00} mode has a Gaussian rotationally symmetric amplitude distribution

$$A(\rho) = A_0 \exp[-\rho^2/\rho_0^2], \tag{2.11}$$

where ρ is the cylindrical coordinate perpendicular to the direction of propagation z and ρ_0 is called the spot radius. The intensity distribution of a Gaussian beam is given by

$$I(\rho) = I_0 \exp[-2\rho^2/\rho_0^2]. \tag{2.12}$$

At $\rho = \rho_0$, the electric field drops to $1/e \cong 37\%$ of its maximum value A_0 while the intensity is reduced to $1/e^2 \cong 14\%$ of I_0. The total power or light flux P_t of a TEM_{00} beam is

$$P_t = 2\pi \int_0^\infty I(\rho)\rho d\rho = \frac{\pi}{2}\rho_0^2 I_0. \tag{2.13}$$

About 86.5% of this flux is contained within a radius equal to the spot radius ρ_0. The laser beam diameter changes during propagation. Thus, except when going through a focus, the wavefronts are not perfectly plane and the spot radius is not constant but a function of z. Since the divergence is inversely proportional to the beam diameter, a sufficiently large spot radius $\rho_0 \gg \lambda$ is a necessary requirement for plane-wave-like behavior.

Short laser pulses are frequently used for grating excitation and detection. If their duration t_p is sufficiently small, the total pulse energy per unit area F, i.e., the exposure or fluence

$$F = \int_{-\infty}^{\infty} I(t)dt \tag{2.14}$$

TABLE 2.1 Physical quantities used for the description of optical fields

	Vacuum	Isotropic material	Anisotropic material
intensity I (plane wave)	$\frac{1}{2}\varepsilon_0 c\lvert E\rvert^2$	$\frac{1}{2}\varepsilon_0 cn\lvert E\rvert^2$	$\frac{1}{\mu_0\omega} E \times (k \times E)$
energy density w	$\frac{1}{2}\varepsilon_0\lvert E\rvert^2$	$\frac{1}{2}\varepsilon_0\varepsilon'\lvert E\rvert^2$	$\frac{1}{2}\varepsilon_0(E \cdot \varepsilon' E^*)$
energy dissipation rate W_f	0	$\frac{1}{2}\varepsilon_0\varepsilon''\omega\lvert E\rvert^2$	$\frac{1}{2}\varepsilon_0\omega(E \cdot \varepsilon'' E^*)$

and the total laser pulse energy

$$W = 2\pi \int_0^\infty F(\rho)\rho d\rho = \int_{-\infty}^{\infty} P_t(t)dt \tag{2.15}$$

are more relevant parameters than the instantaneous quantities intensity and flux.

2.2.2 Superposition of Two Plane Waves

Two-beam interference produces a spatially modulated light field, which is called an interference grating. In many cases, the quantity used for the description of effects related to interference and the interaction with the material is the intensity I. However, in other cases, for a feasible description of the interaction of the interference pattern with the material, the energy density w, or the energy dissipation of the field W_f as introduced in Eq. (2.9) should be used instead [17]. Still in many relevant cases the approximation of the tensor ε'' by a scalar and the assumption of weak absorption are justified, and the three mentioned quantities are proportional to $|E|^2$ (see Table 2.1).

The principal experimental arrangement for the production of laser-induced gratings is shown in Fig. 2.1. Light from a more-or-less powerful pump laser is split into two beams, A and B, with wave vectors k_A, k_B and electric field amplitudes A_A, A_B. The field amplitudes can be written using the polarization vectors p_A, p_B as $A_A = A_A p_A$ and $A_B = A_B p_B$. The two beams intersect at an angle 2θ at the sample and create an interference pattern with an electric field given by

$$E(r,\ t) = \exp(-i\omega t)(A_A \exp[i(k_A \cdot r + \phi_A)] + A_B \exp[i(k_B \cdot r + \phi_B)]). \tag{2.16}$$

Thus,

$$|E(r,\ t)|^2 = A_A^2 + A_B^2 + 2A_A \cdot A_B \cos(K \cdot r + \Delta\phi) \tag{2.17}$$

where the grating vector K and the phase difference $\Delta\phi$ have been introduced, which are given by

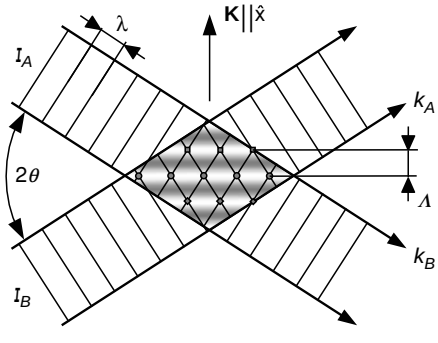

FIGURE 2.1. Interference grating produced by interference of two incident light waves with intensities I_A, I_B and wave vectors k_A, k_B. For simplicity, we have chosen $K \parallel \hat{x}$.

$$\begin{aligned} K &= \pm(k_A - k_B) \\ \Delta\phi &= \pm(\phi_A - \phi_B) \end{aligned} \tag{2.18}$$

The energy density of the field in the material is therefore given by

$$w = (w_A + w_B)\left(1 + \frac{\Delta w}{w_A + w_B}\cos(K \cdot r + \Delta\phi)\right) \tag{2.19}$$

where

$$\Delta w = \varepsilon_0 \varepsilon'(A_A \cdot A_B) \tag{2.20}$$

is the spatial modulation amplitude of the field energy density and w_A and w_B denote the energy densities associated with the incident beams A and B, respectively. To simplify the analysis, we will in the following choose the coordinate system with respect to the grating so that $K \parallel \hat{x}$ and $\phi_A = \phi_B$.

The spatial period of the intensity grating is referred to as Λ and given by

$$\Lambda = 2\pi/K \tag{2.21}$$

where $K = |K|$. Λ can be expressed in terms of the pump wavelength λ and the angle θ.

$$\Lambda = \frac{\lambda}{2\sin\theta}. \tag{2.22}$$

For small angles $\theta \ll 1$, the grating period is approximately

$$\Lambda \approx \lambda/2\theta. \tag{2.23}$$

Note that, up to now, the wave vectors k_A, k_B, the wavelength λ and intersection angle 2θ are measured in the material with refractive index n. For nearly normal incidence, Eq. 2.23 is also approximately valid if the wavelength $\lambda_0 = n\lambda$ and the intersection angle $\theta_0 \approx n\theta$ are measured outside the sample, so that $\Lambda = \lambda_0/2\theta_0$ is obtained as long as $\theta_0 \ll 1$ is satisfied. This means that by varying the intersection angle θ_0, the grating period Λ can be changed. The maximum value of Λ is limited by the diameter of the laser beam inducing the grating. Experimentally, values up to approximately 100μm have been used. The smallest grating-period values are achieved when the two excitation beams are antiparallel with $2\theta = 180^\circ$, giving a minimum value of $\Lambda = \lambda/2 = \lambda_0/(2n)$. Using a visible laser and highly refractive material, the grating period may be smaller than 100 nm.

2.2.3 Superposition of Beams with Different Polarizations

In many textbooks, interference of two plane light waves with parallel polarization is considered [13]. However, excitation of dynamic gratings is also

possible by interfering beams with different, e.g, perpendicular polarization. Therefore, the general case of superposition of beams with different polarization is treated here. This leads to an interference grating with an amplitude described by a tensor.

In most cases, the modulation amplitude of the energy density Δw or the energy dissipation rate ΔW_f are the significant parameters for optical grating creation if both sample and interaction mechanism are isotropic. In anisotropic media, however, or with anisotropic interaction, gratings may also be induced if $p_A \perp p_B$ or $\Delta W_f = 0$. To account for such a situation, we introduce the interference tensor Δm, that is defined as

$$\Delta m_{ij} = \frac{2A_A A_B}{A_A^2 + A_B^2} p_{A,i}\, p_{B,j}, \tag{2.24}$$

where $p_{A,i}$ and $p_{B,j}$ with $i, j = x, y, z$ are the components of the polarization vectors of the incident fields. We can obtain Δw and ΔW_f by evaluating the absolute value of the trace of Δm, e.g.,

$$\Delta w = w_0 |\mathrm{tr}\{\Delta m\}|, \tag{2.25}$$

where $w_0 = w_A + w_B$ is the spatially unmodulated contribution to the field density, so that the spatially dependent field density is then given by

$$w = w_0(1 + |\mathrm{tr}\{\Delta m\}| \cos(Kx)). \tag{2.26}$$

We discuss four important special cases here, which are illustrated in Fig. 2.2:

(a) s polarization: $p_A \parallel p_B \parallel \hat{y}$. This is probably the most frequently used experimental situation and also the simplest one. Δm degenerates into the one-element tensor

$$\Delta m = \frac{2A_A A_B}{A_A^2 + A_B^2} \begin{pmatrix} 0 & 0 & 0 \\ 0 & 1 & 0 \\ 0 & 0 & 0 \end{pmatrix}, \tag{2.27}$$

so that in this case, $\Delta w = 2\sqrt{w_A w_B}$. If, in addition, $A_A = A_B$ then $\Delta w = w_0 = 2w_A$ and

$$w = w_0(1 + \cos Kx). \tag{2.28}$$

Thus, the energy density is fully modulated, varying between zero and four times the value for a single beam.

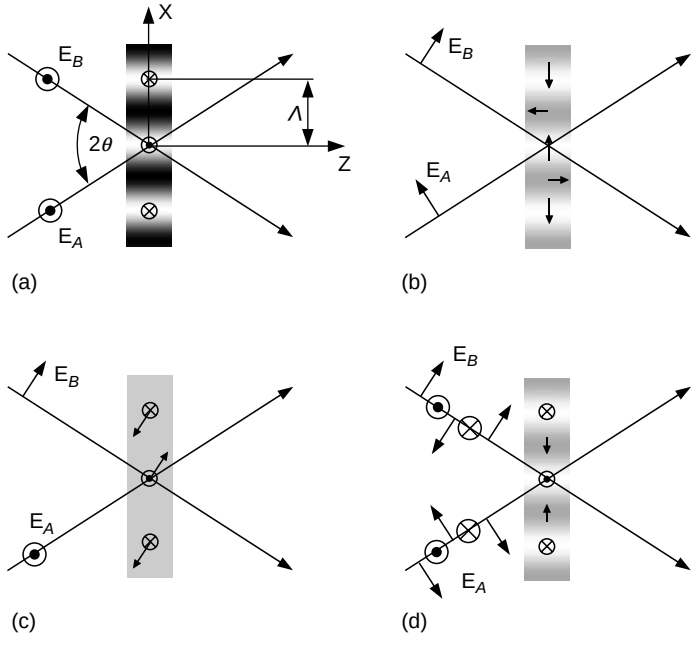

FIGURE 2.2. The four arrangement of pump beam polarizations as discussed in the text. As usual, $\odot$ and $\otimes$ indicate positive and negative directions normal to the paper surface, respectively. The grayscale images illustrate the spatial dependence of the energy density, and the symbols inside indicate the corresponding polarization directions. In (c), the composite symbols indicate vectors that are given by the sum of the two vectors indicated by the individual symbols.

(b) p polarization: $p_A \perp \hat{y}$ and $p_B \perp \hat{y}$. In this case, A_A and A_B are in the xz-plane and the interference tensor is given by

$$\Delta m = \frac{2A_A A_B}{A_A^2 + A_B^2} \begin{pmatrix} p_{Ax}p_{Bx} & 0 & p_{Ax}p_{Bz} \\ 0 & 0 & 0 \\ p_{Az}p_{Bx} & 0 & p_{Az}p_{Bz} \end{pmatrix}, \tag{2.29}$$

which can be written as

$$\Delta m = \frac{2A_A A_B}{A_A^2 + A_B^2} \begin{pmatrix} \cos^2\theta & 0 & \frac{1}{2}\sin(2\theta) \\ 0 & 0 & 0 \\ -\frac{1}{2}\sin(2\theta) & 0 & -\sin^2\theta \end{pmatrix}, \tag{2.30}$$

where 2θ is the angle between the writing beams (see Fig. 2.1), and corresponds to an energy density modulation

$$\Delta w = w_0 |\mathrm{tr}\{\Delta m\}| = 2\sqrt{w_A w_B}(\cos^2\theta - \sin^2\theta). \tag{2.31}$$

The physical interpretation of Δm is as follows: Depending on the relative phase Kx of the two pump beams along x, the superposition of A_A and A_B results in a polarization varying between linear (for $Kx = 0$ and $Kx = \pi$) and elliptic. At $2\theta = 90^\circ$, the intensity modulation disappears completely since $p_A \perp p_B$ in this case. The interference field polarization is particularly interesting if, in addition, $A_A = A_B$. It points into the x-direction for $Kx = 0$, becomes circular at $Kx = \pi/2$, and finally, at $Kx = \pi$, it is linear in the z-direction, i.e., a longitudinal field with respect to the interference pattern (see Fig. 2.2(b)). Interestingly, the polarization interference pattern can be made visible by placing a dichroic medium such as a polaroid foil into the zone of interaction. Thus, for the investigation of optically anisotropic media, perpendicular polarization can be of interest.

(c) Mixed linear polarization: $p_A \parallel \hat{y}, p_B \perp \hat{y}$. In this case, the electric fields of the excitation beams are perpendicular ($A_A \perp A_B$) for any value of θ. The interference tensor is

$$\Delta m = \frac{2A_A A_B}{A_A^2 + A_B^2} \begin{pmatrix} 0 & 0 & 0 \\ p_A p_{Bx} & 0 & p_A p_{Bz} \\ 0 & 0 & 0 \end{pmatrix}. \tag{2.32}$$

No energy density modulation exists. The field amplitude undergoes periodic changes between linear and elliptic polarizations dependent on the relative phase Kx similar to the case of two p-polarized beams with $2\theta = 90^\circ$ discussed before.

(d) Opposite circular polarization with equal amplitudes: In this case, we have $A_A = A_B$ and the polarization vectors of the two beams are given by

$$p_{A,B} = \frac{1}{\sqrt{2}}(\pm \cos\theta \hat{x} + i\hat{y} + \sin\theta \hat{z}). \tag{2.33}$$

The interference tensor is

$$\Delta m = \begin{pmatrix} -\cos^2\theta & i\cos\theta & \frac{1}{2}\sin(2\theta) \\ -i\cos\theta & -1 & i\sin\theta \\ -\frac{1}{2}\sin(2\theta) & i\sin\theta & \sin^2\theta \end{pmatrix}, \tag{2.34}$$

The modulation of the energy density is then

$$\Delta w = 2w_0 \sin^2\theta \tag{2.35}$$

which becomes vanishingly small for $\theta \to 0$, while the polarization tends to become linearly polarized and rotating with the grating period Λ across the grating structure, as indicated in Fig. 2.2(d). This choice of polarization is favorable for studying optically active interactions or media because circular polarization is preserved when a laser beam propagates there.

2.2.4 Superposition of Short Pulses

Present-day mode-locked lasers provide pulses of very short duration, ranging down to the fs regime [18], equivalent to a physical lengths smaller than 0.1 mm. In order to make the beams overlap, sophisticated experimental arrangements have been devoleped [19, 20] The interference of two beams derived from such a source depends on the delay between the pulse fractions traveling along paths A and B. The time dependence of such pulses is close to Gaussian with half width t_p

$$I_{A,B}(t) = \hat{I}_{A,B} \exp\left\{ -\left[\frac{t \pm \tau/2}{t_p}\right]^2 \right\}, \tag{2.36}$$

where τ is the delay of pulse B with regard to A, and $\hat{I}_{A,B} = \frac{1}{2} n c \varepsilon_0 \hat{A}^2_{A,B}$ are the peak intensities of the two pulses. The magnitude of the interference tensor in this case also depends on the overlap of the two pulses given by the ratio τ/t_p, i.e.,

$$\Delta m_{ij} = \frac{2A_A A_B}{A_A^2 + A_B^2} p_{A,i} p_{B,j} \exp\left\{ -\left[\frac{\tau}{2t_p}\right]^2 \right\} \exp\left\{ -\left[\frac{t}{t_p}\right]^2 \right\}. \tag{2.37}$$

Thus, the temporal behavior of $\Delta m(t)$ is the same as that of the original pulse(s), but its amplitude decreases in proportion to $\exp\{-[\tau/2t_p]^2\}$.

2.2.5 Influence of Coherence Properties

Interference of light beams will only be observed as long as the light beams are mutually coherent. Coherence corresponds to the correlation properties between quantities describing the optical field. The temporal coherence function $\Gamma(\tau)$ of a light wave (or light pulse) is defined as the autocorrelation function of the complex field amplitude E

$$\Gamma(\tau) = \int_{-\infty}^{\infty} E^*(t) E(t + \tau) dt. \tag{2.38}$$

The normalized coherence function given by

$$\gamma(\tau) = \frac{\Gamma(\tau)}{\Gamma(0)} \tag{2.39}$$

is used to determine the coherence $|\gamma(\tau)|$ of a laser beam. For an ideal plane wave of monochromatic light, a value of 1 is obtained for all values of τ. For real light sources, the coherence will decrease with increasing $|\tau|$, and the optical coherence length is defined by the width of the coherence function $|\gamma(\tau)|$. The power spectrum of the light G (f) and the absolute value of the coherence

function are related by a Fourier transform relationship, the Wiener–Khintchine theorem [13]

$$G(f) = \int_{-\infty}^{\infty} \gamma(\tau) \exp(i2\pi f \tau) d\tau. \tag{2.40}$$

For a single longitudinal mode laser with Gaussian line shape, the coherence function is given by a Gaussian distribution with its width being inversely proportional to the laser linewidth. For laser light sources with discrete emission frequencies like, e.g., diode lasers in longitudinal multimode operation, the coherence function is more complicated. It is given by a Gaussian envelope with a width determined by the linewidth of a single longitudinal mode, containing oscillations with a spacing inversely dependent on the frequency spacing between the longitudinal laser modes.

It is possible to determine the absolute value $|\gamma(\tau)|$ by measurement of the interference fringe modulation, e.g., using photorefractive index gratings induced by pump and signal beam from the same source and variable optical path delay τ [21]. For the excitation of laser-induced gratings, the optical path length difference of the involved beams must be adapted to the coherence function of the used laser source.

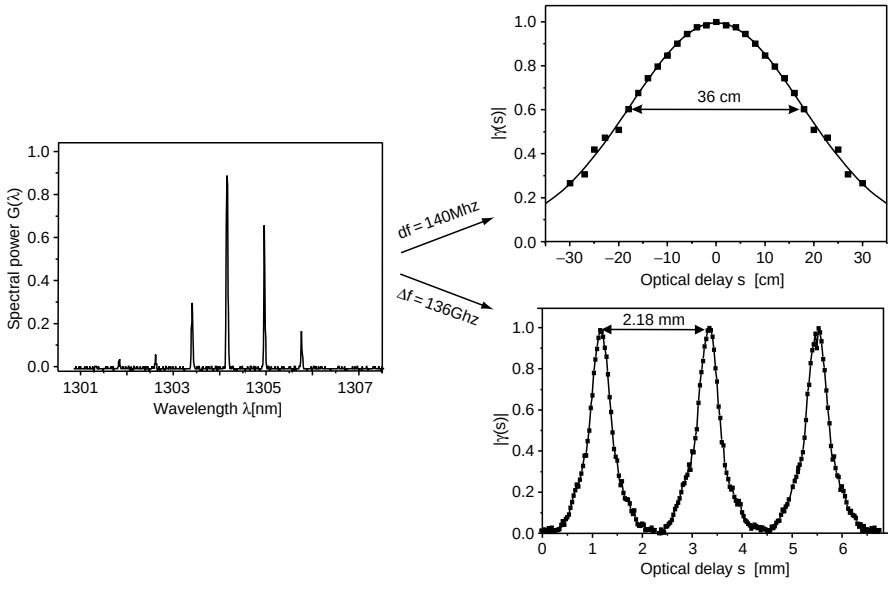

FIGURE 2.3. Relationship between power spectrum (left curve) and coherence function (right curves) of a diode laser. The upper right curve shows the envelope of the coherence function, its width given by the line width of a single longitudinal laser mode df = 140 MHz.The lower right curve shows the modulation contained in the envelope. Spatial periodicity of 2.18 mm corresponds to longitudinal mode spacing of $\Delta\lambda = 0.77$ nm, equivalent to $\Delta f = 136$ GHz. [21]

Note also that the spatial coherence of a laser beam can be determined by diffraction at laser-induced gratings [22]. The spatial coherence function of a Gaussian laser beam with waist ρ_0 is given by

$$\frac{\Gamma(s)}{\Gamma(0)} = \exp\frac{-s^2}{2\rho_0^2}\exp\frac{-\phi_0^2(s)}{2}, \tag{2.41}$$

where $\phi_0^2(s)$ is the mean square change of the phase difference $\Delta\phi$ between two points P_1 and P_2 in a plane normal to the direction of propagation. For a linear dependence $\phi_0^2(s)$, the spatial coherence is also given by a Gaussian function that was indeed observed in the diffraction experiment.

2.2.6 Finite Size Effects

The finite cross-section of the pump-laser beams limits the lateral extent of the interference zone. Hence, the electric-field amplitudes and intensities in Eqs. 2.17–2.20 are slowly varying functions of all spatial coordinates x, y, and z in addition to the modulation with respect to the x-direction. Calculation of the spatial variation is straightforward assuming TEM_{00} beams, but involves a lengthy notation. The interference between two TEM_{00} beams will obviously come close to an ideal plane grating if the following three conditions can be met:

1. The minimum width w of the interaction zone must be large compared to the grating period, i.e.,

$$Kw \gg 1. \tag{2.42}$$

2. The overlap length z_0 of the two beams in z-direction must be large compared to the sample thickness d,

$$z_0/d \gg 1. \tag{2.43}$$

3. The attenuation of the exciting beams must be negligible within the sample, i.e.,

$$\alpha d \ll 1, \tag{2.44}$$

where α is the absorption constant of the material at wavelength λ.

The first condition puts a limit on focusing of the pump beams to increase intensity; the second puts a limit on the angle 2θ between the beams; and the third puts a limit on pump beam utilization by absorption.

The description of a laser-induced grating is particularly straightforward if the above three conditions are satisfied experimentally. In the following discussion, we shall assume this to be the case unless mentioned otherwise.

Note that the results stay qualitatively correct even if one or several of the conditions are satisfied marginally only.

Extremely large values of Λ would require inconveniently small angular beam separations 2θ. Under such circumstances, it is possible to use one pump beam only, and to produce the grating by insertion of a comb-like aperture. Values of Λ up to 4 mm were obtained in this way [23]. There is no obvious upper limit to the period of gratings produced in this manner—except that the laser beam's cross-section has to be increased proportionally, thus lowering the intensity available for the pumping process.

2.2.7 Frequency Offset Effects

The grating is stationary in position when the two beams have the same frequency. When the two excitation beams have slightly different frequencies $\omega_A \neq \omega_B$ and wave vectors k_A and k_B, they can be described by the fields

$$E_i = A_i \exp[i(k_i \cdot r - \omega_i t], \qquad i = A, B, \tag{2.45}$$

where A_A and A_B are the amplitude vectors of the beams, which for simplicity assumed to be parallel. In a region where the beams intersect, an energy density

$$w = \frac{1}{2}\varepsilon_0 \varepsilon'(A_A^2 + A_B^2 + A_A A_B \exp\{i[(k_A - k_B) \cdot r - (\omega_A - \omega_B)t]\}) \tag{2.46}$$

will be created. When deriving this equation, averaging has been performed over times that are long compared to the optical periods of the light fields $2\pi/\omega_A$ and $2\pi/\omega_B$, but short compared to the period $2\pi/(\omega_A - \omega_B)$ corresponding to the difference frequency.

The field energy density w exhibits a wavelike modulation with a grating vector K and a frequency Ω given by

$$K = k_A - k_B \tag{2.47}$$

$$\Omega = |\omega_A - \omega_B|. \tag{2.48}$$

The direction wave vector K is given without the ambiguity that exists in the case of stationary interference patterns. If the material response is fast enough, the frequency offset Ω between the two writing beams will cause traveling grating structures in the material.

2.3 Material Response: Amplitude and Phase Gratings

The mechanisms of light-induced changes of optical materials properties are often described as having two steps. First, the light produces some material excitation, which then leads to a change of the optical properties. In the simplest case, the absorption and the refraction of the material are changed, resulting in amplitude and phase gratings.

Light-induced refractive index changes can in general be referred to as photorefraction. However, the term ''photorefractive effect'' is often used in a more restricted way, describing refractive index changes due to electrooptic effects generated by electric space charge distributions, which are caused by inhomogenous light irradiation, as will be discussed in Section 2.3.6.

2.3.1 Material Excitation Gratings

When a material is placed into the interference region of the pump waves, some light–matter interaction such as absorption creates a corresponding spatial modulation (grating) of some material property [9], e.g., the population of an excited electronic state, the conduction electron density (in a semiconductor [24]), the space charges and their accompanying fields (in photorefractive materials [25]), or the temperature [26] , the molecular orientation (of liquid crystals [27]), or the concentration (in polymer mixtures) [28].

Many of these changes can be described by the population of one, several, or a whole continuum of excited (e.g., electronic or phonon) states of the sample material. Hence, the corresponding gratings can also be considered population gratings in a generalized sense.

The description in terms of excited-state populations is necessary if the local population density is out of thermal equilibrium. This is usually the case if the excited-state energy is far above the thermal energy k_BT, which at room temperature is about 25 meV. Strong deviations from thermal distribution can also occur during radiationless decay from the primarily excited electronic state. In solids, the energy freed during such a process may create hot phonons which, in turn, decay into cooler ones until thermal energies are reached. This process is very fast because hot-phonon lifetimes are on the subpicosecond scale. Since today's mode-locked lasers provide pulses down to femtosecond duration such transient effects can play a role in experiments with extremely high-time resolution. In other materials, it is also possible that long-lived intermediate states of different nature get populated during the decay, particularly at low temperatures. This can considerably slow down the thermalization process, giving rise to secondary grating structures with their own characteristic properties and decay times.

Once the absorbed energy is thermalized locally, the description of the resulting grating in terms of the usual thermodynamic variables, temperature concentration, etc., is appropriate and convenient (compare Fig. 2.4). The sample as a whole is not in equilibrium as long as these quantities still vary spatially. Their equilibration requires transport of heat, matter, etc., which usually occurs by diffusion. Thus, their decay time depends on the magnitude of the excitation gradients, and hence, the K vector of the grating.

Note that a diffusion process, in general, does not change the center position of the excited region but tends to smear out its spatial profile. Hence, a grating stays stationary during diffusive decay, i.e., its phase stays constant while its amplitude decreases monotonically.

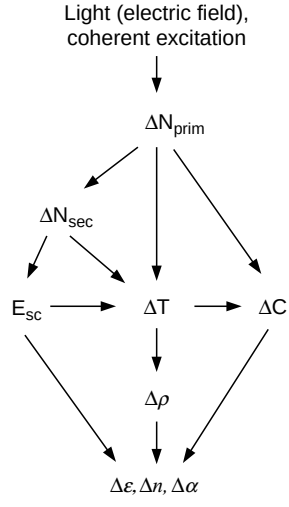

FIGURE 2.4. Possible sequences of material excitations produced by a short laser pulse. N_{prim}, N_{sec}: primary and secondary population density of excited electronic levels, E_{sc}: space charge field, ΔT: temperature change, ΔC: concentration change, $\Delta\rho$: density change, $\Delta\varepsilon$: permittivity change, Δn: refractive index change, and $\Delta\alpha$: absorption change.

The dependence of the material excitation on the light intensity or energy density depends on its dynamics and cannot generally be expressed by a simple function. The time dependence of the material excitation is often described by a differential equation with the pump light intensity as a source term.

Under stationary conditions, the material excitation amplitude ΔX is proportional to the modulated energy density amplitude Δw in the simplest case

$$\Delta X = g^P(\lambda)\Delta w(\lambda), \tag{2.49}$$

where g^P is a coupling coefficient, which depends on the type of material excitation and the pump wavelength λ. The right-hand side may be considered as the first term of a power series describing the general relations between ΔX and Δw. Depending on the nature of excitation, ΔX can be a scalar (temperature, etc.), vector (electric field, flow velocity), or tensor (stress, strain, orientational distribution of excited molecules). Thus, it is convenient for further discussions to rewrite Eq. 2.49 in tensorial form and use the interference modulation tensor Δm

$$\Delta X_{ij} = \sum_{k,l} g^p_{ijkl}\Delta m_{kl}. \tag{2.50}$$

Here i, j, k, l stand for the spatial coordinates x, y, and z. In general, g^p_{ijkl} is a fourth-rank tensor. Note that the tensorial product in Eq. 2.50 allows for a nonvanishing ΔX_{ij} even if $p_A \perp p_B$, i.e., vanishing intensity modulation. Such odd contributions to ΔX_{ij} are needed to account for polarization dependent interactions such as the dichroic bleaching of a dye.

2.3.2 Refractive Index and Absorption Gratings

The material excitation, in general, couples to the refractive index and absorption coefficient, which then also exhibit a grating-like modulation with ampli-

tudes $\Delta n(\lambda)$ and $\Delta\alpha(\lambda)$. Both Δn and $\Delta\alpha$ are, of course, functions of the probe wavelength λ. The refractive-index modulation caused by a temperature grating, for example, is $\Delta n = (\partial n/\partial T)\cdot\Delta T$, where ΔT is the temperature amplitude and $(\partial n/\partial T)$ the thermo-optic coefficient. Generally speaking, any modulation of a material property with amplitude ΔX inside a medium will be accompanied by an optical grating with amplitudes

$$\Delta\alpha = (\partial\alpha/\partial X)\Delta X, \tag{2.51}$$

$$\Delta n = (\partial n/\partial X)\Delta X, \tag{2.52}$$

where the tensor character of ΔX has been ignored for the moment. Quite frequently, one of the coupling constants $(\partial n/\partial X)$ and $(\partial\alpha/\partial X)$ is very small; the grating is then either of the phase or the amplitude type.

Using the complex refractive index $\hat{n}$, the more general expression

$$\Delta\hat{n} = (\partial\hat{n}/\partial X)\Delta X \tag{2.53}$$

is obtained. The complex refractive index $\hat{n}$ is related to the complex optical frequency dielectric constant ε_r and the susceptibility χ by

$$\hat{n} = \sqrt{\varepsilon}_r = \sqrt{1+\chi} \tag{2.54}$$

$$\Delta\hat{n} = \frac{\Delta\varepsilon_r}{2\sqrt{\varepsilon}_r} = \frac{\Delta\chi}{2\sqrt{1+\chi}}. \tag{2.55}$$

Thus, an optical grating corresponds to a spatial modulation of any of the quantities $\hat{n}$, ε_r, or χ. Following Eqs. 2.6 and 2.7, the relation to the refractive index and absorption properties is given by

$$\Delta\varepsilon_r = \Delta\chi = \Delta(\hat{n}^2) = 2n\Delta n + \frac{c^2}{2\omega^2}\alpha\Delta\alpha + i\frac{c}{\omega}(\alpha\Delta n + n\Delta\alpha). \tag{2.56}$$

In many cases, the absorption of the material is weak ($\alpha \ll 2\omega/c$) and the two addends directly proportional to α may be neglected.

2.3.3 Tensor Gratings

It is important that ε_r and χ are tensors, in general, while $\hat{n}$ is not. Therefore, if anisotropic interaction is important, susceptibilities should be used for general description. Specifically, the susceptibility component χ_{ij} connects the electric-field component E_j, with the polarization density component P_i (where again i, j = x, y, z) by means of

$$P_i = \varepsilon_0\chi_{ij}E_j \tag{2.57}$$

$$\Delta P_i = \varepsilon_0\Delta\chi_{ij}E_j. \tag{2.58}$$

The tensorial character of $\Delta\chi_{ij}$ includes induced birefringence and dichroism, i.e., a polarization-dependent refractive index and absorption coefficient. Because both ΔX and $\Delta\chi$ are generally tensors of rank 2, the coupling constant between them is of rank 4, namely,

$$\Delta\chi_{ij} = \sum_{k,l} (\partial\chi_{ij}/\partial X_{kl})\Delta X_{kl}. \tag{2.59}$$

χ_{ij}, $\Delta_{\chi ij}$, and $(\partial_{\chi ij}/\partial X_{kl})$ are generally complex numbers to account for both index of refraction and absorption. Eq. 2.59 shows that the anisotropy of $\Delta\chi_{ij}$ may be either due to the sample medium itself (crystals, external forces, flow), or be induced by the grating formation process. Even in an isotropic solid, anisotropy may be introduced by, e.g., thermal expansion, and namely strain along the direction of K but stress in the planes perpendicular to K. Eq. 2.59 can be combined with Eq. 2.50 to connect the optical grating amplitude directly with the pump field under stationary conditions

$$\Delta\chi_{ij} = \sum_{k,l} f_{ijkl}\Delta m_{kl}, \text{ where} \tag{2.60}$$

$$f_{ijkl} \equiv \sum_{k',l'} (\partial\chi_{ij}/\partial X_{k'l'}) \cdot g^{p}_{k'l'kl}. \tag{2.61}$$

2.3.4 Population Density Gratings in Solids and Liquids

If an atomic system is excited from the ground to an upper state, the absorption coefficient and refractive index change, which can be observed in a grating experiment. In the following, we shall outline some basic equations connecting the intensity of the exciting light field to the change of the optical properties that determine the diffraction properties of the corresponding grating.

Light-induced changes of level population. We will consider simplified atomic systems where the incident light couples only two electronic-energy levels with population densities N_a of the lower level and N_b of the upper level, respectively. The quantity $\Delta N = N_a - N_b$ can be determined by solving the rate equation

$$\frac{\partial N_a}{\partial t} = \frac{N_b}{\tau} - \frac{\sigma wc}{\hbar\omega_0}(N_a - N_b), \tag{2.62}$$

where τ denotes the lifetime of the upper level, σ the absorption cross section, and $\hbar\omega_0$ the energy difference between the involved levels. Note that the product wc corresponds to the intensity I in many cases.

Most of the relevant materials, however, are better described as 3-level-systems in which only two levels are strongly populated. Excitation from the ground state with population density N_0 will create a small population in an intermediate state, that rapidly decays into state with slightly lower energy, having a population density N_1 and a lifetime τ. The rate equation is then

$$\frac{\partial N_0}{\partial t} = \frac{N_1}{\tau} - \frac{\sigma w c}{\hbar \omega_0} N_0. \tag{2.63}$$

In the steady state,

$$\Delta N = N \frac{w/w_s}{1 + w/w_s} \text{ with } w_s = \frac{\hbar \omega_0}{\sigma \tau c}. \tag{2.64}$$

Note that the quantity ΔN will vary spatially with a spatially dependent energy density w, leading to the creation of optical gratings.

Change of optical properties of the material. The 2-level system with transition frequency ω_0 and a half width $1/\tau_{pd}$ of the absorption curve will lead to a polarization density of the material corresponding to a susceptibility [11]

$$\chi = \frac{\mu^2}{\hbar \varepsilon_0} \frac{(N_a - N_b)}{(\omega_0 - \omega) + (i/\tau_{pd})}, \tag{2.65}$$

where τ_{pd} is referred to as polarization decay time or phase relaxation time, and μ denotes the dipole matrix element of the transition. Depending on the ratio $q = (1/\tau_{pd})/|\omega - \omega_0|$, the grating can be approximated by a pure phase grating ($q \gg 1$) or a pure amplitude grating ($q \ll 1$).

Population density gratings have been investigated experimentally in doped crystals (e.g., Cr ions in ruby, Nd ions in YAG) and also in dye solutions [9]. Spatial holes burnt into the upper-level population of laser materials and carrier distribution gratings in semiconductors can also be considered population density gratings. In semiconductors, however, the effects need to be described using spatially dependent equations as transport mechanisms for the carriers need to be taken into account.

2.3.5 Gratings in Semiconductors

In solid state crystals like semiconductors, the electronic-energy levels are not discrete with respect to their energy like in single atoms. Instead these levels are contained in several energy bands, and their density within these bands, referred to as density of states ρ, is dependent on their associated energy E. Most relevant to the description of the optical properties of semiconductors are the valence band and the conduction band, which are separated by a band gap energy $E_g = E_c - E_v$, where E_c is the lowest and E_v the highest possible energy in the respective bands. Close to this band gap, the density of states for electrons in the conduction band can be approximated by

$$\rho_c(E) = \frac{(2m_c)^{3/2}}{2\pi^2 \hbar^3} \sqrt{E - E_C}, \tag{2.66}$$

where m_c denotes the effective mass of an electron in the conduction band when moving within the lattice. Please note that here and throughout this section, similar expressions are obtained for the quantities related to the valence band, but will be omitted as the relationships for the conduction band are sufficient to understand the concepts of the model. If needed, quantities related to the valence band will be denoted using the subscript v rather than c for the conduction band without further notice.

In thermal equilibrium, the probability that an electronic state is actually taken by an electron is given by the Fermi function f_c of the conduction band

$$f_c(E) = \frac{1}{\exp[(E - F_c)/k_B T] + 1}, \tag{2.67}$$

where k_B denotes the Boltzmann number and F_c denotes the Fermi energy of the conduction band. This Fermi energy determines the electron density in the conduction band N_c by the integral

$$N_c = \int_{E_c}^{\infty} \rho_c(E)\, f_c(E)\, dE, \tag{2.68}$$

and vice versa.

Each electronic state given by a certain wave function is also associated with a certain momentum $\hbar k$. While in general the relation between the associated energy and wave number k of a state can be quite complicated; we will limit our discussion to electronic states close to the band gap where the relationship

$$\hbar k = \sqrt{2m_c(E - E_c)} \tag{2.69}$$

holds. The density of states is approximately given by $\rho(k) = k^2/\pi^2$ in both the valence and conduction bands. The conservation of momentum $\hbar k$ needs to be considered in processes like optical transitions.

Optical transitions in semiconductors. Absorption of light leads to transitions of the electrons so that excited states are populated. The polarizability of the excited electrons is different from the ground-state polarizability, similar to the situation described in Section 2.3.4. In semiconductors, the transitions may take place from the valence to the conduction band (interband transitions) or within a band (intraband transitions).

The density of systems N_b in the excited state can be obtained from solving a suitable rate equation describing the generation and recombination processes

$$\frac{\partial N_b}{\partial t} = \frac{\sigma w c}{\hbar \omega}(N_a - N_b) - \frac{N_b}{\tau}. \tag{2.70}$$

Here τ is the recombination time, σ the absorption cross-section of the transition, and N_a the density of systems in the ground state. Note that there may be several decay mechanisms involved that can make it necessary to replace the

recombination rate N_b/τ by a more complicated relationship, like a Taylor expansion $AN_b + BN_b^2 + CN_b^3 + \ldots$, where the coefficients A, B, C are attributed to different decay mechanisms, e.g., intraband relaxations. For small light intensities, the density of excited electrons is obtained as

$$\frac{N_b}{N_a + N_b} = \frac{\sigma\tau wc}{\hbar\omega}. \tag{2.71}$$

In semiconductors, there are also grating decay mechanisms, that may not be described solely by time-dependent equations. Diffusion of the carriers involved will cause a spatially dependent current density J_{diff}, that may significantly contribute to the carrier grating that is eventually obtained and, especially in experiments with pulsed laser sources, its lifetime.

Carrier diffusion. Because of the spatial gradient of the electron density, diffusion processes will occur and create a current density of the electrons

$$J_{diff} = qD\nabla N_c, \tag{2.72}$$

where D is the diffusion constant of the material, which in general is a tensor quantity, and $q = \pm e$ the charge of the carrier. The holes will create a corresponding diffusion current. The spatially dependent rate equation is then

$$\frac{\partial N_b(x,\ t)}{\partial t} = \frac{\sigma cw\,(x,\ t)}{\hbar\omega}\ (N_a - N_b) - \frac{N_b(x,\ t)}{\tau} + \frac{1}{q}\nabla \cdot J_{diff}(x,\ t). \tag{2.73}$$

Note that in this case, it becomes possible that the maximum of the light field modulation will be spatially separated from the maximum number of excited carriers. We will discuss such effects in Section 2.3.6.

The modulated carrier densities lead to corresponding changes of the optical properties, thereby forming a grating. We will limit our discussion of the grating creation to two effects: the bleaching of the interband absorption and the absorption caused by free carriers in the bands.

Bleaching of the interband absorption. In direct semiconductors, interband transitions lead to a depletion of the absorbing electrons in the valence band. In addition, the density of the unpopulated energy states in the conduction band is reduced. The wave number of the electronic states is determined by the conservation of momentum and by the band structure as

$$\hbar k(\omega_0) = \sqrt{2m_r(\hbar\omega_0 - E_g)}\ , \tag{2.74}$$

where ω_0 is the frequency of the light wave, and $m_r = (1/m_c + 1/m_v)^{-1}$ is the reduced effective mass of the electron-hole pair (see Fig. 2.5). Electrons within an interval of width Δk around this wave number may be involved in the transition, because the energy of the involved states is also known within a certain interval only (due to the uncertainty principle). This energy interval is determined by intraband relaxation processes as $\Delta E = \hbar/\tau_{relax}$.

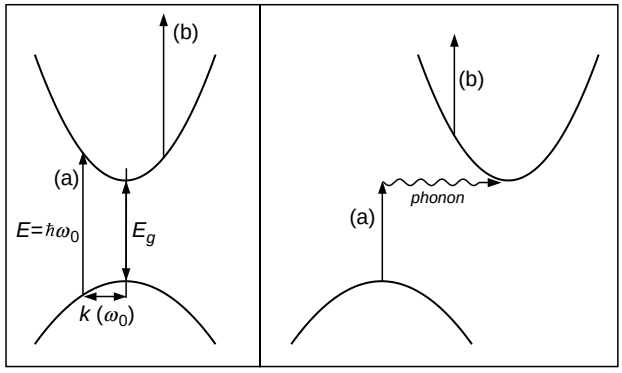

FIGURE 2.5. Optical transitions in direct (left image) and indirect (right image) semiconductors. The curves shown indicate the electron energy of the valence band (lower curve) and conduction band, respectively, as a function of the wavenumber k. Interband transitions (denoted with letter (a)) can take place if $\Delta k = 0$ in the direct semiconductor, or involving a phonon in the indirect semiconductor material. Intraband absorption of free carriers is denoted with letter (b).

The density of the states for each of the levels involved may be expressed as

$$N = \rho(k)\, f(k)\, \Delta k \tag{2.75}$$

so that the difference $(N_a - N_b)$ of the populations of the two states with their respective energies E_a, E_b can be expressed as

$$N_a - N_b = \frac{(2m_r)^{3/2}}{\pi \hbar^2 \tau_{relax}} \sqrt{\hbar\omega - E_g}\,(f_c(E_b) - f_v(E_a)) \tag{2.76}$$

and the change of the absorption constant $\Delta\alpha(\omega) = \sigma(N_a - N_b)$ can be calculated.

The change of the absorption coefficient is accompanied by a change of the refractive index Δn. It is possible to estimate Δn using the Kramers–Kronig relation [29].

$$\Delta n = \frac{c}{\pi} \int_0^\infty \frac{\Delta\alpha(\omega')}{\omega'^2 - \omega^2}\, d\omega'. \tag{2.77}$$

The change of the absorption coefficient and the refractive index can be combined to express a change of the complex susceptibility. From Eq. 2.56 with $\alpha \ll 2\omega/c$, we obtain

$$\Delta\varepsilon_r(\omega) = 2n\Delta n + i\frac{nc}{\omega}\Delta\alpha. \tag{2.78}$$

Free-carrier absorption. In indirect band-gap semiconductors like silicon, the absorption of radiation at a frequency corresponding to the band-gap energy does not lead to absorption bleaching. On the contrary, the absorption increases due to transitions within the conduction and valence bands. The frequency dependence of the corresponding change of the permittivity ε_r may be approximately described by the classical Drude model that treats the electrons and holes as quasifree carriers oscillating in the light field [30]

$$\Delta\varepsilon_r(\omega) = \frac{Ne^2}{\varepsilon_0 m_r \omega(\omega + i/\tau_{relax})^2}. \tag{2.79}$$

Here N is the population density of the optically excited electron–hole pairs and τ_{relax} is the relaxation time.

2.3.6 Photorefractive Gratings in Electro-Optic Crystals

The photorefractive effect is caused by free carriers, which are released due to ionization of donors or acceptors in electro-optic materials. The light driving the effect has an optical frequency ω smaller than $E_g/\hbar$, because the energy of these so-called photorefractive centers is situated within the band-gap. Important examples for photorefractive electro-optic crystals are $LiNbO_3$, $BaTiO_3$, KNSBN, or $Sn_2P_2S_6$. We will limit our discussion to a single center model, with a single trap level, acting as a donor, and electrons as carriers. For deeper understanding of many photorefractive materials, more sophisticated models are needed [31].

Like in semiconductors, a spatially dependent carrier distribution is created by the light field. The corresponding space charge ρ creates an electric field E_{sc}. Apart from its influence to carrier transport processes, this field is responsible for the change of the ε_r tensor by means of the electro-optic effect.

2.3.6.1 Generation and Recombination Processes

The generation and recombination processes are described by the densities N_D and N_D^+ of the donor atoms and the ionized donor atoms, respectively, and by the density of the electrons in the conduction band N_c by the rate equation

$$\frac{\partial N_D^+}{\partial t} = \left(\frac{\sigma cw(x,\ t)}{\hbar\omega} + \beta\right)(N_D - N_D^+) - \gamma_R N_c N_D^+, \tag{2.80}$$

where β is a rate constant describing the thermal excitation, and γ_R denotes the recombination constant. Note that the ionized donors cannot change positions, while the electrons will create a current density J, so that the rate equation for the electron density is

$$\frac{\partial N_c}{\partial t} = \frac{\partial N_D^+}{\partial t} + \frac{1}{e}\nabla \cdot J. \tag{2.81}$$

2.3.6.2 Transport Phenomena

The current density J consists of three important contributions. The creation of a diffusion current density J_{diff} has already been discussed in Section 2.3.5. Here, we have two other important contributions: drift currents induced by an electric field obtained as the sum of an initrinsic space charge field, and an external electric field applied to the material and photovoltaic currents.

Drift. The spatially dependent carrier concentration causes a space charge field E_{sc}. This intrinsic electric field and a possibly externally applied field E_{ext} will add up, and create a current density

$$J_{drift} = qN_c\mu_c(E_{sc} + E_{ext}), \tag{2.82}$$

where μ_c denotes the mobility of the electrons. For the holes, an equivalent correlation applies. The diffusion constant and the mobility are related by $D = \mu_c k_B T/q$.

Photovoltaic effect. In piezoelectric materials, photoelectrons are excited into the charge transfer band with a preferential direction of the velocity along the direction of the polar axis. Additional current contributions due to anisotropic electron trapping and ion displacement are also possible. The current density is given by

$$J_{ph} = -\beta_{ijk}E_j E_k^*. \tag{2.83}$$

The overall current density is given by $J = J_{diff} + J_{drift} + J_{ph}$.

2.3.6.3 Space Charge Field and Electro-Optic Effect

The space charge field induced by the carrier distribution will satisfy Maxwell's equation

$$\nabla \cdot (\varepsilon E) = \rho \tag{2.84}$$

and can be determined from the space charge distribution using the Coulomb law for anisotropic media [32]. For $\rho = \rho_0 \cos(K \cdot r)$ as the first harmonic component of the space charge distribution induced by the energy density modulation in the material created by the incident light waves, the integration leads to [6]

$$E_{sc} = \rho_0 \frac{K}{K \cdot \varepsilon K} \sin(K \cdot r) = E_1 \cos(K \cdot r - \pi/2), \tag{2.85}$$

where $E_1 \parallel K$ has been introduced as the amplitude of the space charge field. The phase shift of $\pi/2$ means that the space charge field is spatially shifted by $\Lambda/4$ with respect to the energy density modulation, as indicated in Fig. 2.6. When no external field is applied to the material (diffusion-driven effect), the

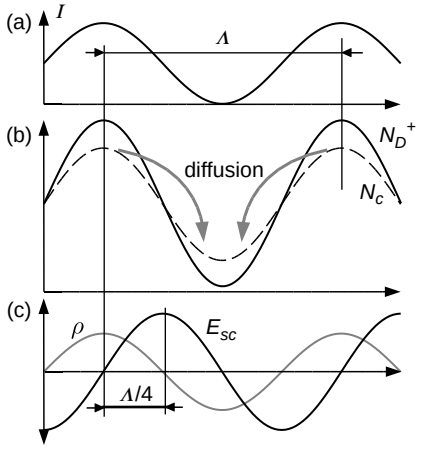

FIGURE 2.6. Photorefractive grating build-up: (a) the stationary intensity pattern with grating constant Λ, (b) distribution of ionized donors N_D^+ and electrons N_c. The latter distribute by diffusion. (c) The resulting space charge distribution ρ induces a space charge field E_{sc}, spatially shifted by $\Lambda/4$.

amplitude E_1 of the electric field can be obtained [6], using the interference tensor Δm as

$$E_1 = \frac{2\pi}{\Lambda}\frac{k_B T}{q}\left(1+\frac{l_D^2}{\Lambda^2}\right)^{-1}|\mathrm{tr}\{\Delta m\}|, \tag{2.86}$$

where l_D denotes the Debye screening length of the material.

The modulation of the dielectric tensor caused by the electro-optic effect caused by an electric field E can be written as

$$(\Delta\varepsilon_r)_{ij} = -n_i^2 n_j^2 (r_{ijk}E_k + s_{ijkm}E_k E_m) \tag{2.87}$$

where r_{ijk} and s_{ijkm} denote the components of the tensor quantities describing the material properties for the first-order and second-order electro-optic effect, and E_k and E_m denote components of E. The magnitude of the components of these tensors for a single material may vary significantly, which implies that the strength of the photorefractive effect can vary considerably with the orientation of the grating vector K, e.g., in $BaTi0_3$ (and other crystals with the same point group symmetry, 4 mm) the modulation of the permittivity change due to the electric field E_1 is given by

$$\Delta\varepsilon_r(E_1) \equiv \varepsilon_1 = -\begin{pmatrix} n_o^4 r_{13}E_{1z} & 0 & n_o^2 n_e^2 r_{42}E_{1x} \\ 0 & n_o^4 r_{13}E_{1z} & n_o^2 n_e^2 r_{42}E_{1y} \\ n_o^2 n_e^2 r_{42}E_{1x} & n_o^2 n_e^2 r_{42}E_{1y} & n_e^4 r_{33}E_{1z} \end{pmatrix} \tag{2.88}$$

where n_o and n_e are the ordinary and extraordinary indices of refraction, and the r_{ij} correspond to the material coefficients r_{ijk} used in Eq. 2.87 in a shortened notation. For the equation above, we have chosen that the crystal

axis (also referred to as the c axis) is parallel to the z direction. As the coefficient r_{42} is by far the largest in $BaTi0_3$, the effect is strongly anisotropic and because the grating vector K and therefore also the vector E_1 are in the x–z-plane, the field component E_{1x} is the most significant one.

2.4 Grating Detection by Diffraction and Wave-Mixing

Diffraction at dynamic or permanent gratings is a special problem in the more general context of light-matter interaction. It can be treated by different theoretical descriptions with varying levels of sophistication, in which certain assumptions simplifying the problem are made. For example, it is possible to predict the diffraction angles correctly using simple geometrical considerations about the constructive or destructive interference of partial waves created by the gratings (see Section 2.4.1). In order to obtain information about the amplitudes of the diffracted waves, solutions of the wave equation are obtained for special cases by the Fraunhofer Diffraction theory or the Coupled Mode Theory (see Section 2.4.2). Effects causing energy transfer between the involved partial waves are referred to as wave mixing, where the probably most important examples are Two-Wave Mixing (discussed in Section 2.4.3), and Four-Wave mixing that can lead to the creation of optical gratings acting as a phase-conjugate mirror.

2.4.1 Diffraction Angles

Gratings are usually divided into several subclasses. Probably, the most important distinction is between thin and thick gratings. The latter are often also referred to as volume gratings.

Thin gratings. A light-wave incident at a thin periodical structure (a thin grating) will produce a number of partial waves that may at a certain distance from the grating interfere in a constructive or destructive manner, dependent on the difference between their respective optical path lengths.

From geometrical considerations (see Fig. 2.7(a)), the familiar condition for the directions of constructive interference, given by the diffraction angles φ_m

$$\Lambda[\sin(\theta + \varphi_m) - \sin(\theta)] = m\lambda, \quad m = 0, \pm 1, \pm 2, \ldots \tag{2.89}$$

is obtained, where θ denotes the angle of incidence, λ the wavelength of the light, and Λ the spatial period of the grating. For sufficiently small angles θ, φ_m, the angle of mth order of diffraction is given by

$$\varphi_m = m\frac{\lambda}{\Lambda} \tag{2.90}$$

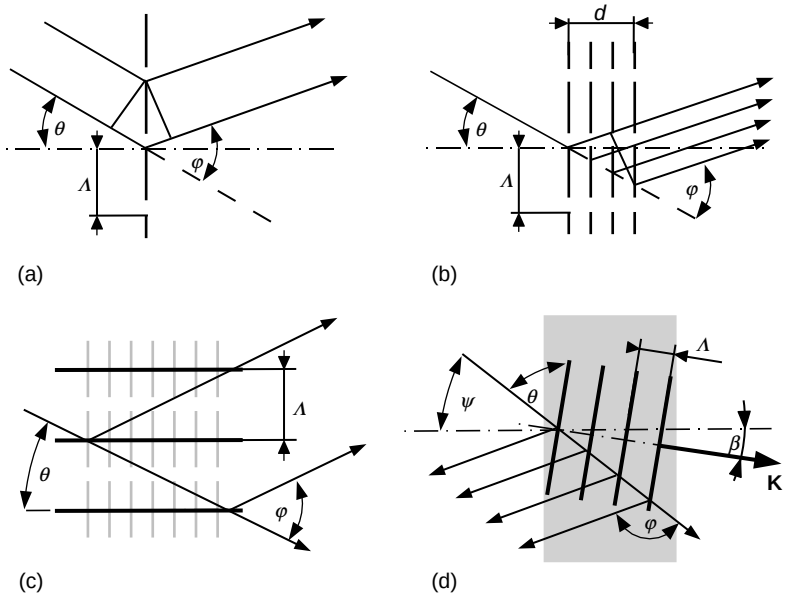

FIGURE 2.7. Diffraction at a single thin grating (a), at a series of thin gratings (b), at a thick (volume) transmission grating (c), and at a reflection volume grating (d). Incidence angle is denoted as θ, diffraction angle as φ and grating period as Λ.

and, there, the angular separation between two adjacent diffraction orders is approximately constant at a value λ/Λ. For $K \parallel \hat{x}$, the x-component of the wave vectors k_m of the diffraction orders are given by

$$k_{m,x} - k_x = mK \quad m = 0, \pm 1, \pm 2, \ldots, \tag{2.91}$$

where k_x denotes the x-component of the wave vector of the incident wave.

When the diffracting structure is thicker than a certain value, partial waves created within different depths have to be in phase as well in order to observe constructive interference. To estimate up to which thickness existing phase differences may be neglected, the structure may be described as a succession of a number of thin-grating structures (see Fig. 2.7(b))

The optical path difference Δs between partial waves originating from thin-grating elements separated by a thickness d is given by

$$\Delta s = d(1 - \cos\varphi)/\cos\theta. \tag{2.92}$$

For small angles θ and φ that satisfy Eq. 2.90, the corresponding phase difference $\Delta\phi$ is given by

$$\Delta\phi = 2\pi \frac{\lambda d}{\Lambda^2 n(1 - \theta^2)}. \tag{2.93}$$

This means that at normal incidence, the phase difference will be sufficiently small ($\Delta\phi \ll 1$), if the grating thickness satisfies

$$\mathrm{d} \ll \frac{\Lambda^2 \mathrm{n}}{2\pi\lambda}. \tag{2.94}$$

Thick gratings. If the condition for a thin grating given by Eq. 2.94 is not satisfied, the partial waves that are diffracted at angles according to Eq. 2.89 at different depths must be exactly in phase in order to interfere constructively. This leads to a condition for the incidence angles at which diffracted beams can be observed. Deriving Eq. 2.94, we have neglected that every partial beam is diffracted at a subgrating that appears to be spatially shifted by a distance $\Delta\mathrm{x} = \mathrm{d}\tan\theta$. The Fourier transform diffraction theory for thin gratings (see Section 2.4.2) shows that the diffracted beam will have a phase shift $\Delta\phi = 2\pi\Delta\mathrm{x}/\Lambda$ with respect to a beam diffracted at the untranslated grating. Following Eq. 2.92, the resulting phase difference is then given by

$$\Delta\phi = 2\pi\frac{\mathrm{d}\tan\theta}{\Lambda} - \frac{\mathrm{d}(1-\cos\varphi)}{\cos\theta}\frac{2\pi}{\mathrm{m}\lambda}. \tag{2.95}$$

The condition $\Delta\phi = 0$ and Eq. 2.89 describing the diffraction at the thin subgratings can only be simultaneously fulfilled if $\varphi = -2\theta$ and, therefore

$$2\sin\theta = 2\sin\left(-\frac{\varphi_\mathrm{m}}{2}\right) = \frac{\mathrm{m}\lambda}{\Lambda}, \quad \mathrm{m} = 0, \pm 1, \pm 2, \ldots \tag{2.96}$$

This equation is referred to as the Bragg condition, and indeed in the experiment it can be verified that only one diffraction order is created from a volume grating, and only if the incidence angle is chosen according to Eq. 2.96. Note that the condition $\varphi = -2\theta$ is also obtained if the diffracted waves are interpreted as reflections at planes formed by the structures of the thin subgratings, as is illustrated in Fig. 2.7(c).

Using the wave vectors of the incident and the diffracted light waves, the Bragg condition may be expressed as

$$\mathrm{k}_\mathrm{m} - \mathrm{k} = \mathrm{mK}, \quad \mathrm{m} = 0, \pm 1, \pm 2, \ldots. \tag{2.97}$$

Diffraction at a thick grating requires that all components of the wave vectors involved satisfy conditions, in contrast to a thin grating, where only one component of the wave vector is determined by the diffraction (compare Eq. 2.91). The configuration shown in Fig. 2.7(c) is referred to as a transmission volume grating. When the incidence angle θ exceeds $\pi/4$ as shown in Fig. 2.7(d), the grating is called a reflection volume grating. Here the grating vector K has a slant angle β with respect to the z-axis. Note that the Bragg condition is valid for the angle $\theta = (\pi/2 - (\psi - \beta))$ for this configuration.

2.4.2 Diffraction Amplitudes and Efficiencies

In order to gain information about the amplitudes of the diffracted waves, solutions to the Helmholtz equation

$$\nabla^2 E(x,z) + k^2 \varepsilon_r(x,z) E(x,z) = 0, \tag{2.98}$$

where we have restricted our analysis to the x–z-plane, can be found using different approaches. For thin gratings, the well-known classical boundary-value approach of Huyghens and Kirchhoff may be used. For thick gratings, the wave propagation inside the material has to be considered. For weakly modulated gratings, a suitable approach is the coupled-wave theory in the two-wave approximation as described by Kogelnik [33].

Fourier transform diffraction theory for thin gratings. Based on the assumption that the light is linearly polarized, Eq. 2.98 is reduced to a scalar equation for the one-dimensional field amplitude E. The thin grating will change the incident wave

$$E^{(i)} = A^{(i)} \exp[i(\omega t - kz)] \tag{2.99}$$

into the following wave by means of its transmittance $t(x)$

$$E(z=0) = A^{(i)} t(x) \exp[i(\omega t)], \tag{2.100}$$

where, for simplicity, normal incidence has been assumed. The transmittance can be calculated from the spatially modulated permittivity ε_r. The wave behind the grating is described by a superposition of plane waves with amplitudes A_m as

$$E = \sum_m A_m \exp[i(\omega t - k_m x - \sqrt{k^2 - k_m^2}\, z)]. \tag{2.101}$$

Substituting Eq. 2.91 into this equation we obtain

$$A_m = \frac{A^{(i)}}{\Lambda} \int_0^{\Lambda} t(x) \exp(i2\pi \frac{mx}{\Lambda}) dx \tag{2.102}$$

which means that the wave amplitudes A_m are given by the Fourier coefficients of the transmittance $t(x)$. The diffraction efficiency for the mth diffraction order is given by $\eta_d = (A_m/A^{(i)})^2$.

For the case of a sinusoidal refractive index grating, the transmission function can be written as

$$t(x) = \exp[i\phi \cos(2\pi x/\Lambda)], \tag{2.103}$$

where $\phi = 2\pi\Delta\hat{n}d/\lambda$ is determined by the modulation amplitude $\Delta\hat{n}$ of the refractive index grating. For a pure amplitude transmittance grating (i.e., $\mathrm{Re}(\hat{n}) = 0$), only the three central diffraction orders (corresponding to $m = 0, \pm 1$) are observed [34], and a maximum diffraction efficiency of $\eta_d = 6.25\%$ is obtained for the first order $m = \pm 1$. In contrast, a pure phase grating will diffract into higher orders as well. The maximum diffraction efficiency for the first order is $\eta_d = 33.8\%$ for a value of the grating amplitude $\phi \approx 1.8$.

Coupled-wave theory for volume gratings. For a volume grating with slant angle β between grating wave vector K and the surface normal of the material (compare Fig. 2.7(d)), the spatial modulation of material properties may be written as

$$\varepsilon_r(x,\ z) = \varepsilon_c + \varepsilon_1 \cos\left(K(x \sin\beta + z\cos\beta)\right) \tag{2.104}$$

A slant angle $\beta = 0$ corresponds to an unslanted reflection grating, $\beta = \pi/2$ to an unslanted transmission grating. We can substitute

$$E = \sum_m A_m \exp\left[i(k_i - mK)\cdot r\right] \tag{2.105}$$

into the wave equation, and applying the approximation of weak absorption ($\varepsilon_r - n^2 \approx in\alpha/k$) and neglecting the second-order derivative d^2A_m/dz^2 (which is known as the slowly varying envelope (SVE) approximation), we obtain the rigorous coupled-wave equations [9]

$$\begin{aligned} i\left(\cos\psi - \frac{m\lambda\cos\beta}{n\Lambda}\right)\frac{dA_m}{dz} + m\frac{\pi}{\Lambda^2}\left(2\Lambda\cos(\psi-\beta) - m\frac{\lambda}{n}\right)A_m \\ + i\frac{\alpha}{2n}A_m + \frac{\pi n\varepsilon_1}{2\lambda}(A_{m+1} + A_{m-1}) = 0 \end{aligned} \tag{2.106}$$

which is an infinite set of coupled differential equations. The real-valued coefficient of the first addend proportional to A_m will vanish only for the transmitted wave $m = 0$ and the one mth partial wave that satisfies the Bragg condition given in Eq. 2.96. For all other waves, the nonvanishing coefficient leads to oscillatory behavior with respect to the propagation direction z, a continuous build-up of the amplitude A_m is not possible. This corresponds to the statement that (if any) only one diffracted-wave may be generated efficiently by a volume grating. We will therefore reduce the coupled-wave equations in Eq. 2.106 to only two equations, for the two waves given by amplitudes A_0 and A_1. In this two-wave approximation, using the definitions

$$\kappa = \frac{\pi\varepsilon_1}{2n\lambda\cos\psi} \tag{2.107}$$

$$\delta = \frac{\alpha}{2\cos\psi} \tag{2.108}$$

we obtain the equations

$$\begin{aligned} \frac{dA_0}{dz} &= -\delta A_0 + i\kappa A_1 \\ \pm\frac{dA_1}{dz} &= -\delta A_1 + i\kappa A_0. \end{aligned} \tag{2.109}$$

These equations cover two cases: the plus sign in the second equation corresponds to the unslanted transmission grating case ($\beta = \pi/2$). For an unslanted reflection grating ($\beta = 0$), the minus sign applies. The quantity κ used in the equations is referred to as the coupling constant. It will take a slightly different form when the coupling between waves of different polarization is to be described.

Let the polarization of two waves be given by the two polarization vectors p_1, p_2, and the amplitude of the spatial modulation of the permittivity be given by the tensor quantity ε_1 to account for anisotropy, the coupling constant takes the form [6]

$$\kappa_{ij} = \frac{\pi}{2n_i\lambda\cos\psi_i\varepsilon_0} p_i \cdot \varepsilon_1 p_j, \tag{2.110}$$

where $i, j = 1, 2$. Note that two waves that are both polarized within the plane of incidence have different polarization vectors and Eq. 2.110 needs to be used rather than Eq. 2.107 obtained from the scalar wave equation [33].

Transmission volume gratings. The initial condition for solving the Eqs. (2.109) for a transmission grating is given by the amplitudes $A_0(0)$ and $A_1(0)$ when entering the interaction region, and the solution is given by

$$\begin{aligned} A_0(z) &= (A_0(0)\cos(\kappa z) + iA_1(0)\sin(\kappa z))\exp(-\delta z) \\ A_1(z) &= (A_1(0)\cos(\kappa z) + iA_0(0)\sin(\kappa z))\exp(-\delta z). \end{aligned} \tag{2.111}$$

When a single beam is incident on the grating, the initial conditions are $A_0(0) = A^{(i)}$ and $A_1(0) = 0$. The dependence of the intensities on the position is depicted in Fig. 2.8. Because the absorption of the material is considered to be weak, we may then use Eq. 2.78 to compute the amplitude and phase grating amplitudes, and the diffraction efficiency of a grating of thickness d is obtained as

$$\eta_d(d) = \frac{I_1}{I^{(i)}} = \left(\sin^2\frac{\pi\Delta n d}{\lambda\cos\psi} + \sinh^2\frac{\Delta\alpha d}{4\cos\psi}\right)\exp[-2\delta d]. \tag{2.112}$$

Reflection volume gratings. In the reflection case, the Bragg condition causes the diffracted wave to travel into the region in front of the grating, while behind the grating region, only the transmitted beam corresponding to diffraction order $m = 0$ is observed. Therefore, the diffracted beam is often referred to as a reflected beam.

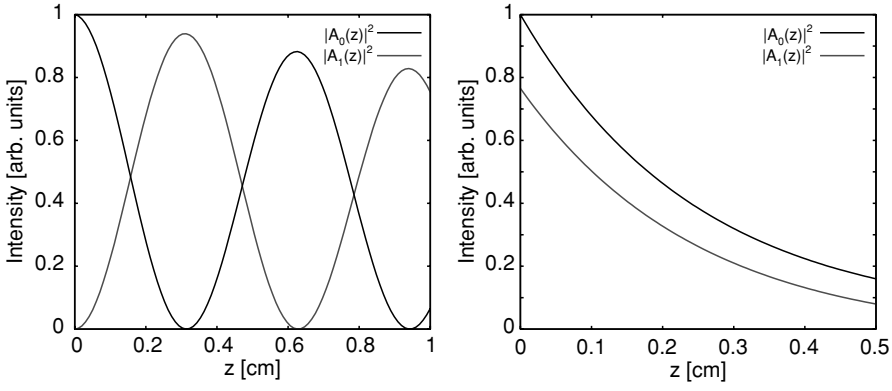

FIGURE 2.8. Diffraction at volume gratings: Calculated normalized field densities for an incidence angle $\psi = 10^\circ$, assuming an absorption coefficient $\alpha = 0.5\,\mathrm{cm}^{-1}$ and a phase-only transmission grating with $\kappa = 4\,\mathrm{cm}^{-1}$ (left figure) and a reflection grating with $\kappa = 2\,\mathrm{cm}^{-1}$ (right figure), respectively.

Assuming a volume grating of thickness d, the initial conditions are determined by the wave amplitudes $A_0(0)$ and $A_1(d)$ as the beams enter the interaction region from opposite directions. The solutions in this case are obtained as

$$A_0(z) = A_0(0)\left(\cosh(\zeta z) - \frac{\delta}{\zeta}\sinh(\zeta z)\right) + iB\frac{\kappa}{\zeta}\sinh(\zeta z) \tag{2.113}$$

$$A_1(z) = B\left(\cosh(\zeta z) + \frac{\delta}{\zeta}\sinh(\zeta z)\right) - iA_0(0)\frac{\kappa}{\zeta}\sinh(\zeta z) \tag{2.114}$$

where we have introduced ζ and B as

$$\zeta = \sqrt{\kappa^2 + \delta^2}, \tag{2.115}$$

$$B \equiv A_1(0) = \frac{iA_0(0)\kappa\sinh(\zeta d) + \zeta A_1(d)}{\zeta\cosh(\zeta d) + \delta\sinh(\zeta d)} \tag{2.116}$$

and identified the quantity B as the amplitude of the reflected wave at the boundary $z = 0$. For a single wave incident on the grating $A_1(d) = 0$ and neglecting the bulk material absorption ($\alpha = 0$), we obtain the diffraction efficiency η_d of a pure phase grating ($\Delta\alpha = 0$) as

$$\eta_d = \tan h^2\frac{\pi\Delta n d}{\lambda\cos\psi}. \tag{2.117}$$

2.4.3 Two-Wave Mixing in Electro-Optic Crystals

In this section, we will discuss the interaction of laser beams with the grating that has been induced in a material due to the spatial modulation of their intensity I, energy density w, or energy dissipation rate W_f, using the two-wave mixing in electro-optic crystals as an example. At a light-induced grating written by two writing beams A and B, each of the beams will be partially transmitted (with amplitudes $A_{A,0}$ and $A_{B,0}$) and partially diffracted (with amplitudes $A_{A,1}$ and $A_{B,1}$). The transmitted part of one beam happens to be collinear with the diffracted part of the other beam and vice versa. As the beams A and B are coherent (for simplicity we will assume ideal coherence here), the field amplitudes of the respective transmitted and diffracted beams will add up.

Depending on the material, the light field will produce a material excitation and produce a modulation of the permittivity that can be approximately described by

$$\varepsilon_r(x,\ z) = \varepsilon_c + \varepsilon_1 \cos(K \cdot r + \phi), \tag{2.118}$$

where ϕ describes a spatial shift between the stationary field modulation and the induced optical grating that can be caused by the physical mechanism of grating creation. In a diffusion-driven photorefractive material without external field, we have $\phi = \pi/2$ as obtained in Eq. 2.85.

The modulation amplitude ε_1 of the dielectric tensor is dependent on the interference tensor of the incident writing beams, i.e.,

$$\varepsilon_1 = |\mathrm{tr}\{\Delta m\}|\tilde{\varepsilon}_1 \tag{2.119}$$

as can be seen from Eqs. 2.86 and 2.88 for the case of electro-optic crystals. As diffraction will change the amplitudes of the writing beams (and consequentially the interference tensor Δm) while they propagate through the material, following the discussion of transmission volume gratings in Section 2.4.2 and Eq. 2.24, the case of codirectional two-wave mixing can be described by a set of coupled differential equations for the beam intensities I_A and I_B

$$\begin{aligned} \frac{dI_A}{dz} &= \gamma \frac{I_A I_B}{I_A + I_B} - \delta I_A \\ \frac{dI_B}{dz} &= -\gamma \frac{I_A I_B}{I_A + I_B} - \delta I_B, \end{aligned} \tag{2.120}$$

where the coupling constant

$$\gamma = \frac{\pi p_A \cdot p_B}{n\lambda \cos\psi \varepsilon_0} (p_A \cdot \tilde{\varepsilon}_1 p_B) \sin\phi \tag{2.121}$$

has been introduced. When there is no spatial shift between the stationary field modulation and the induced optical grating (i.e., $\phi = 0$), the coupling coefficient is zero, while it reaches a maximum for $\phi = \pm\pi/2$. As can be seen from its definition, the orientation of the polarization vectors of the beams with respect to each other and to the crystal axes is significant for the magnitude of γ. Following Eq. 2.88, we obtain for a wave mixing of beams with polarization vectors $p_A = (p_{Ax},\ p_{Ay},\ p_{Az})$ and $p_B = (p_{Bx},\ p_{By},\ p_{Bz})$ in $BaTiO_3$

$$(p_A \cdot \tilde{\varepsilon}_1 p_B) \propto r_{42} \sin\xi (p_{Ax}p_{Bz} + p_{Az}p_{Bx}), \tag{2.122}$$

where the c-axis of the crystal is again assumed to be parallel to the z direction, and the K vector of the grating is contained in the x–z-plane with an angle ξ to the c axis. In Eq. 2.122, we have only considered the contribution of the dominant nonlinear coefficient r_{42}, and it can be seen that only beams with a polarization parallel to the x–z-plane (i.e., e–o polarized beams in this case) will create a significant coupling coefficient γ. In order to determine the incidence angles so that the largest value of γ can be obtained, the influence of material parameters (e.g., the Debye screening length, compare Eq. 2.86) as well as the limit to the interference contrast given by $p_A \cdot p_B$ need to be considered.

The solution of Eq. 2.120 is found as

$$\begin{aligned} I_A(z) &= I_A(0)\frac{1 + m^{-1}}{1 + m^{-1}\exp(\gamma z)}\exp(-\delta z) \\ I_B(z) &= I_B(0)\frac{1 + m}{1 + m\exp(-\gamma z)}\exp(-\delta z), \end{aligned} \tag{2.123}$$

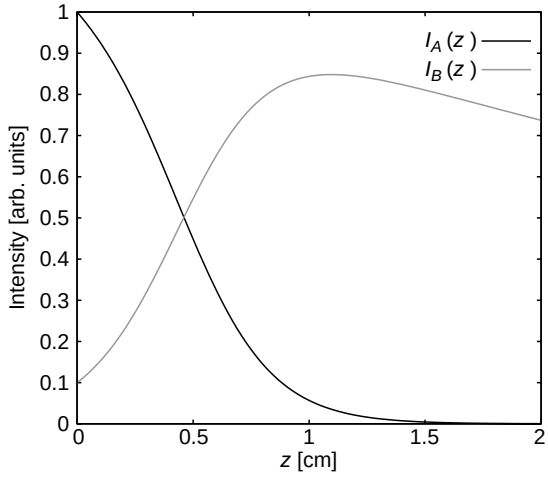

FIGURE 2.9. Calculated intensities of the writing beams in the interaction region of a two-wave mixing process assuming $m = 10$, $\gamma = 5\,cm^{-1}$ and $\delta = 0.2\,cm^{-1}$. After an interaction length of 1 cm, beam B has reached maximum intensity.

where $m = I_A(0)/I_B(0)$ denotes the input intensity ratio of the two beams. In Fig. 2.9, it can be seen that the intensity of one of the beams may be almost fully transferred into the other beam, only limited by the material absorption.

2.5 Conclusions

Dynamic gratings can be induced by interfering laser beams in almost any optical material. Some selected works related to laser-induced gratings have been used as references of this chapter, but inevitable these publications cover only a small fraction of the research activities in this widespread field. There are certainly many other important contributions that we could not include here. The following chapters of this volume are devoted to the photorefractive materials and will provide a detailed review of the effects related to this important class of materials, in particular, of the effects related to laser-induced gratings in photorefractive materials.

Acknowledgments

We would like to thank Prof. G. Montemezzani from the University of Metz, France and some unknown referee for review and fruitful discussion of this chapter.

References

1. H.J. Coufal, D. Psaltis, and G.T. Sincerbox, eds.: Holographic data storage, Vol. 76 of Springer Series in Optical Sciences, Springer, New York (2000).
2. H.J. Eichler, P. Kuemmel, S. Orlic, and A. Wappelt: High density disk storage by multiplexed microholograms, IEEE J. Selected Topics Quantum Electron. 4(5), 840–848 (1998).
3. D.C. Meisel, M. Wegener, and K. Busch: Three-dimensional photonic crystals by holographic lithography using the umbrella configuration: Symmetries and complete photonic band gaps, Phys. Rev. B, 70, 165104 (2004).
4. A. Brignon and J.-P. Huignard, eds.: Phase conjugated laser optics, John Wiley & Sons (2004).
5. T. Riesbeck, E. Risse, and H.J. Eichler: Pulsed solid-state laser systems with high brightness by fiber phase conjugation, Proc. SPIE 5120, pp. 494–499, Nov. 2003.
6. P. Yeh, Introduction to photorefractive nonlinear optics, Wiley 1993.
7. L. Solymar, DJ. Webb, and A. Grunnet-Jepson: The physics and applications of photorefractive materials, Oxford University Press (1996).
8. A.A. Zozulya: Propagation of light beams in photorefractive media: Fanning, self-bending and formation of self-pumped four-wave-mixing phase conjugation geometries, Phys. Rev Lett. 73 (6), 818–825 (1994).

9. H.J. Eichler, P. Günter, and D.W. Pohl: Laser-induced dynamic gratings, Springer-Verlag, Berlin (1986).
10. O. Svelto: Principles of lasers, Kluwer Academic/Plenum Publishers (1998).
11. A. Yariv: Quantum electronics, John Wiley & Sons, 3rd edn (1989).
12. A. Yariv and P. Yeh: Optical waves in crystals, John Wiley & Sons (1984).
13. M. Born and E. Wolf: Principles of optics, Cambridge University Press, 7th edn. (1999).
14. L. Bergmann and C. Schäfer: Optics of waves and particles, De Gruyter (1999).
15. G.N. Ramachandran and S. Ramaseshan: Crystal optics, Vol. XXV/1 of Handbuch der Physik, Springer-Verlag, Berlin (1961).
16. P. Günter, ed.: Nonlinear optical effects and materials, Vol. 72 of Springer Series in Optical Sciences. Springer, Berlin (2000).
17. G. Montemezzani, C. Medrano, and M. Zgonik: Charge carrier photoexcitation and two-wave mixing in dichroic materials, Phys. Rev. Lett. 97, 3403–3406 (1997).
18. M. Nisoli, S.D. Silvestri, R. Scipocs, K. Ferencz, C. Spielmann, S. Sartania, and F. Krausz: Compression of high-energy laser pulses below 5fs, Opt. Lett. 22(8), 522(1997).
19. A.A. Mahznev, T.F. Crimmins, and K.A. Nelson: How to make femtosecond pulses overlap, Opt. Lett. 23 (17), 1378–1380 (1998).
20. I.Z. Kozma and J. Hebling: Comparative analysis of optical setups for excitation of dynamic gratings by ultrashort light pulses, Opt. Commun. 199, 407–415 (2001).
21. P. Pogany, A. Hermerschmidt, S.X. Dou, and H. J. Eichler: Simple measurement of the temporal coherence function of cw diode lasers by a photorefractive grating method, in 5th International Workshop on Laser Beam and Optics Characterization, H. Weber and H. Laabs, eds., pp. 71–78, March 2000.
22. H.J. Eichler, G. Enterlein, and D. Langhans: Investigation of the spatial coherence of a laser beam by a laser-induced grating method, Appl. Phys. 23, 299–302 (1980).
23. C. Allain, H.Z. Cummins, and P. Lallemand: Critical slowing down near the Rayleigh–Benard convective instability, J. Physique Lett. 39, L475–L479 (1978).
24. T. Sjodin, H. Petek, and H.-L. Dai: Ultrafast carrier dynamics in silicon: A two-color transient reflection grating study on a (111) surface, Phys. Rev Lett. 81 (25) 5664–5667 (1998).
25. M. Sudzius, R. Aleksiejunas, K. Jarasiunas, D. Verstraeten, and J.C. Launay: Investigation of nonequilibrium carrier transport in vanadium-doped CdTe and CdZnTe crystals using the time-resolved four-wave mixing technique, Semicond. Sci. Technol. 18 (4), 367–76 (2003).
26. P.F. Barker, J.H. Grinstead and R.B. Miles: Single-pulse temperature measurement in supersonic air flow with predissociated laser-induced thermal gratings, Opt. Commun. 168, 177–182 (1999).
27. M. Jazbinšek, I.D. Olenik, M. Zgonik, A.K. Fontecchio, and G.P. Crawford: Characterization of holographic polymer dispersed liquid crystal transmission gratings, J. Appl. Phys. 90 (8), 3831–3837 (2001).
28. M.J. Escuti, J. Qi, and G.P. Crawford: Two-dimensional tunable photonic crystal formed in a liquid–crystal/polymer composite. Threshold behavior and morphology, Appl. Phys. Lett. 83 (7) 1331–1333 (2003).
29. E. Garmire and A. Kost, eds: Nonlinear optics in semiconductors I, Vol. 58 of Semiconductors and Semimetals, Academic Press, San Diego (1999).
30. T. Numai: Fundamentals of semiconductor lasers, Vol. 93 of Springer Series in Optical Sciences. Springer, New York (2004).

31. K. Buse: Light-induced charge transport processes in photorefractive crystals, I: Models and experimental methods, II: Materials, Appl. Phys. B 64, 273–291, 391–407 (1997).
32. B. Jancewicz: A variable metric electrodynamics. The Coulomb and Biot-Savart laws in anisotropic media, Ann. Phys. 245, 227–274 (1996).
33. H. Kogelnik: Coupled-wave theory for thick hologram gratings, Bell Syst. Tech. J. 48, 2909–2948 (1969).
34. J.W. Goodman, Introduction to Fourier optics, McGraw-Hill, 2nd ed. (1996).